

# A Method For Monitoring Deposition at a Solid Cathode in an Electrorefiner for a Two- Species System Using Electrode Potentials

**Global 2013**

D. S. Rappleye  
M. F. Simpson  
R. M. Cumberland  
M. -S. Yim

**October 2013**

This is a preprint of a paper intended for publication in a journal or proceedings. Since changes may be made before publication, this preprint should not be cited or reproduced without permission of the author. This document was prepared as an account of work sponsored by an agency of the United States Government. Neither the United States Government nor any agency thereof, or any of their employees, makes any warranty, expressed or implied, or assumes any legal liability or responsibility for any third party's use, or the results of such use, of any information, apparatus, product or process disclosed in this report, or represents that its use by such third party would not infringe privately owned rights. The views expressed in this paper are not necessarily those of the United States Government or the sponsoring agency.

The INL is a  
U.S. Department of Energy  
National Laboratory  
operated by  
Battelle Energy Alliance



# A METHOD FOR MONITORING DEPOSITION AT A SOLID CATHODE IN AN ELECTROREFINER FOR A TWO-SPECIES SYSTEM USING ELECTRODE POTENTIALS

D. S. Rappleye<sup>a</sup>, M. F. Simpson<sup>b</sup>, R. M. Cumberland<sup>c</sup>, and M.-S. Yim<sup>c</sup>

<sup>a</sup>*Department of Nuclear Engineering, North Carolina State University, Box 7909 Raleigh, NC 27695  
E-mail: drapple@ncsu.edu*

<sup>b</sup>*Center for Advanced Energy Studies, Idaho National Laboratory, P.O. Box 1625, Idaho Falls, ID 83415*

<sup>c</sup>*Department of Nuclear and Quantum Engineering, Korea Advanced Institute of Science and Technology, 291 Daehak-ro, Yuseong-gu, Daejeon, Korea*

*Currently, process monitoring of spent nuclear fuel electrorefining relies upon sampling and destructive analysis methods coupled with extrapolative thermodynamic process models for non-interrupted operations. Corrections to those models are performed infrequently, jeopardizing both the control of the process and safeguarding of nuclear material. Furthermore, the timeliness of obtaining the results is inadequate for application of international safeguards protocol. Alternatively, a system that dynamically utilizes electrical data such as electrode potentials and cell current can hypothetically be used to achieve real-time process monitoring and more robust control as well as improved safeguards. Efforts to develop an advanced model of the electrorefiner to date have focused on a forward modeling approach by using feed and salt compositions to determine the product composition, cell current and electrode potential response. Alternatively, an inverse model was developed, and reported here, to predict the product deposition rates on a cathode using the cell current, cathode potential, and fundamental relations of electrochemistry. The model was applied to the following cases: pure uranium deposition, co-deposition of uranium and plutonium, and co-deposition of uranium and zirconium. The deposition rates predicted by the inverse model were compared to those of a forward model, ERAD.*

## I. INTRODUCTION

Pyroprocessing is a promising spent nuclear fuel (SNF) reprocessing technology because of its ability to process high enriched, short cooled fuel; its compact space requirements; its intrinsic inability to separate pure plutonium (Pu); and its production of waste streams immediately suitable for permanent disposal. However, certain features of pyroprocessing complicate the task of process monitoring and optimization.

Two complicating features are lack of input accountability and large material hold-up. SNF assemblies are the feed for pyroprocessing and vary in composition spatially. The assemblies are disassembled, chopped, and placed in an electrorefiner (ER), where uranium (U) and other actinides are oxidized from the spent fuel into a molten salt electrolyte and U is reduced onto a solid cathode. Unlike in aqueous reprocessing technologies such as PUREX and COEX, the fuel does not completely dissolve at any step within the process. This prevents the operator from taking a sample that would be representative of the fuel feed. However, Pu and other transuranic elements do oxidize and accumulate in the molten salt with each batch of fuel processed. The inventory of actinides cannot be accurately calculated from a mass balance because of the uncertainty in the feed. Thus, measurement methods are required to monitor the buildup of actinides in the molten salt. These measurements would support the tasks of managing criticality safety, ensuring product quality, and performing nuclear material accountancy.

Electroanalytical techniques utilizing electrode probes (cyclic voltammetry, square wave voltammetry, etc.) have shown promise in making quantitative measurements of the elemental composition of molten salts. However, there are several problems with this approach yet to be solved, including limited concentration ranges, difficulty in calculating baselines, interference between different actinides, and lack of knowledge of key physical parameters (diffusivity, activity coefficients, etc.). Alternatively, monitoring the process settings and measurements could provide information regarding molten salt and product composition, but this requires an accurate process model.

Process monitoring of the Fuel Condition Facility (FCF) at Idaho National Laboratory (INL) uses a mass

tracking system (MTG) which tracks the location and inventory of items as they pass from unit to unit in the process.<sup>1</sup> The FCF consists of multiple units of operation including two electrorefiners, two fuel choppers, a cathode processor, and a casting furnace.<sup>2</sup> In units, such as the ER, in which the inventories of items are partitioned into separate product phases, the changes in item compositions and masses are modeled using the MTG. The modeling of the ER in MTG is based on a thermodynamic model.<sup>2, 3</sup> The model predictions are either verified or updated by sampling and destructive analysis (DA) upon availability and the MTG is subjected to replays to update process inventories. However, the DA of molten salt sample usually takes several weeks. This delay could result in the process being operated at non-optimal settings for prolonged periods of time and create timeliness issues for material accountability.

An alternative approach would be to continue to track items in the process as currently done using the MTG, but to add functionality for the real-time analysis of process signals. These could include electrode potentials, cell current, temperature, power fed to motors and ER heaters, and density. Using individual process readings or a combination of those signals, the compositions and process dynamics could be predicted via calculation. In order for this approach to be successful, a chemically and physically accurate and dynamic model of the ER is needed.

Several dynamic models of electrorefiners have been developed. A co-operative effort undertaken by INL, KAERI, and Seoul National University (SNU) resulted in the development of comprehensive two- and three-dimensional model of the Mark-IV. KAERI and SNU developed the three-dimensional model, which coupled a three-dimensional computational fluid dynamics (CFD) model with an electrochemical reaction model (REFIN).<sup>4</sup> In parallel, University of Idaho (UI) and INL developed a two-dimensional model of the Mark-IV.<sup>6</sup> The model calculated potential and current distributions for U, Zr and Pu for a horizontal cross-section of the ER, essentially assuming no vertical variations. In addition to the efforts of INL, KAERI, UI, and SNU, another comprehensive model of the Mark-IV has been developed by Li et. al.<sup>7</sup> Li uses a three-dimensional CFD model which calls a FORTRAN model to calculate and set the boundary conditions based on electrochemical calculations. The model accounts for four species: U, Pu, Nd and Zr.

ER modeling has not been limited to the Mark-IV system. Lee et. al. modeled the KAERI ER geometry in an aqueous system processing copper.<sup>8</sup> This model uses ANSYS-CFX to generate electric field distributions and particle flow patterns. Also, a general model to predict the critical current or bulk uranium concentration at which

co-deposition of Pu begins in an ER was developed at Los Alamos National Laboratory (LANL).<sup>9</sup> ERAD (Enhanced REFIN with Anodic Dissolution) is a general one-dimensional ER model that can be applied to arbitrary ER configurations by adjusting various geometric parameters such as electrode areas and diffusion boundary layer thicknesses.<sup>10</sup> ERAD performs particularly well in the geometric configuration of concentric cylinders. It is important to note that due to the one-dimensionality of ERAD, a uniform potential distribution is assumed.

ERAD was developed by modifying REFIN in a number of ways. A model was added to describe the dissolution of SNF from a solid anode, solubility limits were enforced at the anode surface, geometry of the anode was altered to account for a porous layer of noble metals,<sup>11</sup> the differential equation solver was replaced, and a package was inserted to account for fast reactions occurring before the application of an external power source. ERAD has the capability to account for up to 10 elements counting those present in the eutectic LiCl-KCl melt. ERAD's calculations were compared to experimental data from CRIEPI.<sup>12</sup> ERAD demonstrated good agreement in electrode potentials, but it over-predicted rate of Pu transport and under-predicted rate of U transport. In addition, the time of Zr dissolution commencement did not agree with the experimental data. The code is currently undergoing further validation against cyclic voltammetric data.<sup>10</sup>

A commonality among these models is that they are forward models.<sup>a</sup> The forward models use the composition of the feed material and salt to predict the electrochemical responses of the system and, in some cases, the product composition. However, as discussed, these compositions may not be readily available. Thus, the use of an inverse model, which uses the electrochemical responses to predict the salt and product compositions, could be more suitable for the real-time analysis of process signals. Such an inverse model was developed based on electrochemical theory. The theoretical model was developed to use cathode potentials and cell current to provide rapid feedback on the cathode deposition rates of species in the ER. Calculations were made using this model for the cases of pure uranium deposition, U/Pu co-deposition and U/Zr co-deposition. The resulting deposition rates are compared to the ERAD simulations of the same cases.

---

<sup>a</sup> The LANL model has some inverse solving capability in that it solves for a critical bulk uranium concentration at a given cell current, but does not provide composition predictions.

## II. ANALYSIS OF CATHODE DEPOSITION

An approach was developed to use cathode potential measurements at varying current levels to estimate the instantaneous deposition rate of each species at any given time based on electrochemical theory. To illustrate this approach, an example is given for a system in which two-species are actively being reduced at the cathode. In such a system, the cell current would be stepped to different values. Figure 1a shows an example of a cell current profile for this procedure. At first, the ER is at its normal operating current, then dropped to zero briefly, then slightly elevated for a moment and finally returned to operating conditions. When this current cycle is applied, a corresponding cathode potential profile would be measured (see Figure 1b).

A key assumption to this method is that the bulk concentrations of the elements in molten salt are constant. This assumption is valid if the amount of an element reduced during the cycle is significantly less than amount present in the salt. The scenario of greatest concern would be when a species with trace amounts in the salt accounts for a significant amount of the deposition at the cathode.

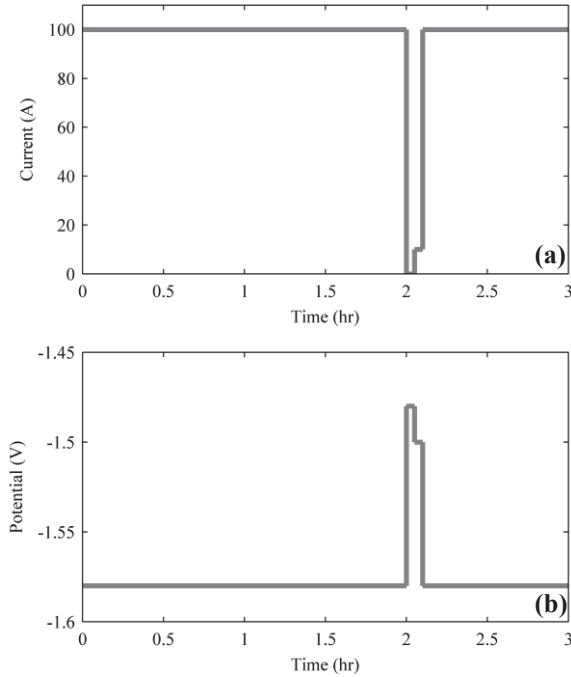


**Figure 1** Example current (a) and potential (b) profile for two-species deposition

### II.A. Model Development

A model was developed to demonstrate this approach of estimating deposition rate. The initial development of

this model stems from the work by Park.<sup>5</sup> As applied to the reactions occurring at the cathode with simplified notation and taking the cathodic current as positive, the following form of the Butler-Volmer equation is used.

$$I_{j,k} = i_{o,j} \left[ \frac{a_{s,j}^{ox}}{a_{b,j}^{ox}} e^{-\frac{(1-\alpha_j)n_j F}{RT}(\eta_{j,k})} - \frac{a_{s,j}^{red}}{a_{b,j}^{red}} e^{\frac{\alpha_j n_j F}{RT}(\eta_{j,k})} \right] \quad (1)$$

$I_{j,k}$  is the partial current of species  $j$  at step  $k$ ,  $i_o$  is the exchange current,  $a_b^{ox}$  is the activity of the oxidized species in bulk molten salt,  $a_b^{red}$  is the activity of the reduced species in the bulk cathode,  $a_s$  is the activity at the surface of the cathode,  $\alpha$  is the transfer coefficient,  $F$  is Faraday's constant,  $R$  is the universal gas constant,  $n$  is the number of electrons transferred,  $T$  is the cell temperature and  $\eta$  is the overpotential. The exchange current in Eq. (1) is given by:

$$i_{o,j} = i_{o,j}^o A \left( a_{b,j}^{ox} \right)^{\alpha_j} \left( a_{b,j}^{red} \right)^{1-\alpha_j} \quad (2)$$

where  $A$  is the electrode surface area. The following equation defines the overpotential in Eq. (1):

$$\eta_{j,k} = E_k - E_{eq,j} \quad (3)$$

where  $E$  is the electrode potential at current setting,  $k$ , and  $E_{eq}$  is the equilibrium potential. The equilibrium potential is given by the Nernst equation:

$$E_{eq,j} = E_j^o - \frac{RT}{n_j F} \ln \left( \frac{a_{b,j}^{red}}{a_{b,j}^{ox}} \right) \quad (4)$$

where  $E^o$  is standard reduction potential. In an ER, the reduced species is in a solid phase and its activity is assumed to be unity. The formula for the activity of the oxidized species expressed in terms of concentration is:

$$a_j^{ox} = \gamma_j^{ox} x_j^{ox} = \gamma_j^{ox} \frac{c_j^{ox}}{c_{tot}} \quad (5)$$

where  $\gamma$  is the activity coefficient,  $c$  is the concentration in the molten salt,  $x$  is the mole fraction in molten salt,  $c_{tot}$  is the total concentration of the molten salt mixture and is initially approximated to be the concentration of eutectic LiCl-KCl at 500°C.

By combining Eqs.(1) – (5) and simplifying, the following expression is obtained.

$$I_{j,k} = i_{o,j}^o A \left[ \gamma_j^{\text{ox}} \frac{c_{s,j}^{\text{ox}}}{c_{\text{tot}}} e^{-\frac{(1-\alpha_j)n_j F}{RT}(E_k - E_j^o)} - e^{\frac{\alpha_j n_j F}{RT}(E_k - E_j^o)} \right] \quad (6)$$

The surface concentration term can be eliminated by using a mass-transfer relation, such as:

$$I_{j,k} = n_j F A h_j (c_{b,j}^{\text{ox}} - c_{s,j}^{\text{ox}}) \quad (7)$$

where  $h$  is the mass-transfer coefficient. An expression, Eq. (8), for current is obtained that is a linear function of bulk concentration by solving Eq. (7) for the bulk concentration and substituting into Eq. (6).

$$I_{j,k} = \frac{i_{o,j}^o A \left[ \gamma_j^{\text{ox}} \frac{c_{b,j}^{\text{ox}}}{c_{\text{tot}}} e^{-\frac{(1-\alpha_j)n_j F}{RT}(E_k - E_j^o)} - e^{\frac{\alpha_j n_j F}{RT}(E_k - E_j^o)} \right]}{\frac{i_{o,j}^o \gamma_j^{\text{ox}} e^{-\frac{(1-\alpha_j)n_j F}{RT}(E_k - E_j^o)}}{n_j F h_j c_{\text{tot}}} + 1} \quad (8)$$

In Eq. (8), there are two unknowns,  $c_{b,j}^{\text{ox}}$  and  $E_k$ . The rest are species' properties, general constants or parameters that are known or can be determined.

As shown in Figure 1, the ER current is adjusted to different settings and the potential of the cathode is measured at each setting. This eliminates one unknown,  $E_k$ , and supplies a constraint, Eq. (9), which uses the cell current at each current setting.

$$I_k^{\text{cell}} = \sum_j I_{j,k} (c_{b,j}^{\text{ox}}, E_k) \quad (9)$$

Thus, the number of current settings,  $k$ , needs to be equivalent to the number of unknown species,  $j$ , reacting at the cathode.

As noted, Eq. (8) is linear with respect to bulk concentration. Thus a code was written in Visual Basics for Applications (VBA) which solves the system of linear equations for the co-deposition of two elements. Additionally, a user interface was developed for the VBA code in Microsoft Excel 2007.

In developing the model, certain parameters needed to be estimated, specifically the mass transfer coefficients and total concentration. The mass transfer

coefficients were determined by dividing the diffusion coefficients by the diffusion layer thickness,  $\delta$ .

$$h_j = \frac{D_j}{\delta_j} \quad (10)$$

As shown in Table I,  $\delta$  is assumed to be 50  $\mu\text{m}$ . This assumed value for the diffusion layer can be illustrated using the following relation for a rotating cylindrical electrode:<sup>13</sup>

$$\delta_j = 12.64 \frac{d^{0.30} \nu^{0.344} D_j^{0.356}}{\omega^{0.70}} \quad (11)$$

where  $d$  is diameter of the electrode,  $\nu$  is the kinematic viscosity of the electrolyte and  $\omega$  is peripheral velocity at the electrode surface. The kinematic viscosity of eutectic LiCl-KCl was calculated to be 0.013  $\text{cm}^2/\text{s}$  using reported viscosity and density measurements.<sup>14</sup> Considering the Mark-V ER design where electrode diameters are approximately 25 cm (Ref. 15), the assumed diffusion layer thickness could be produced at a rotational rate of 80 rpm. This illustration demonstrates that, in order to apply this model to a specific ER, an accurate mass transfer correlation for the geometry of the electrodes and information regarding electrode diameter and rotational rate are required.

As mentioned, the total concentration is initially set to 29.02 mol/L, the concentration of LiCl-KCl.<sup>6</sup> However, once the concentrations of the other constituents are calculated, the moles of the other constituents are subtracted from the moles of the LiCl-KCl. For example, consider the following balances:



If the amount of chlorine in the salt is fixed then, for every mole of metal,  $M$ , in the salt  $x$  moles of LiCl-KCl are replaced to maintain electroneutrality. Thus, the initial moles of LiCl-KCl are adjusted as shown below:

$$\text{mol}_{\text{LiCl-KCl}} = \text{mol}_{\text{LiCl-KCl}}^o - \sum_j^m x_j \text{mol}_{M_j} \quad (14)$$

where  $m$  is the total number of species concentrations calculated by the model and  $\text{mol}^o$  is initial amount of moles. This results in a closer approximation to the total concentration. Using Eq. (14), the error of total concentration estimated by the model was at maximum

7.5% and on average 3.6 % of the total concentrations calculated by ERAD. The error introduced by this approximation would be exacerbated by an accumulation of significant amounts of elements that are non-reactive at the cathode.

Additionally, a method was developed to identify whether a species was co-depositing with U. This method is illustrated in Figure 2. Initially only U deposition is assumed to occur at the cathode. Under this assumption, the bulk concentration of U ( $C_U$ ) is calculated using the open-circuit potential (OCP) of the cathode and Eq. (4) as applied to electrodeposition of U metal.

$$E_{eq,U} = E_U^o + \frac{RT}{n_U F} \ln \left( \gamma_U^{ox} \frac{C_U^{ox}}{C_{tot}} \right) \quad (15)$$

Using the calculated  $C_U$ , the current of U ( $I_U$ ) at the operational potential ( $E_{OP}$ ) is predicted. If  $I_U$  and the ERAD calculated cell current ( $I_{cell}$ ) at operating conditions matched within a certain tolerance, then it was concluded that only U was depositing at the cathode. However, if the currents did not match, then another species was assumed to be depositing.

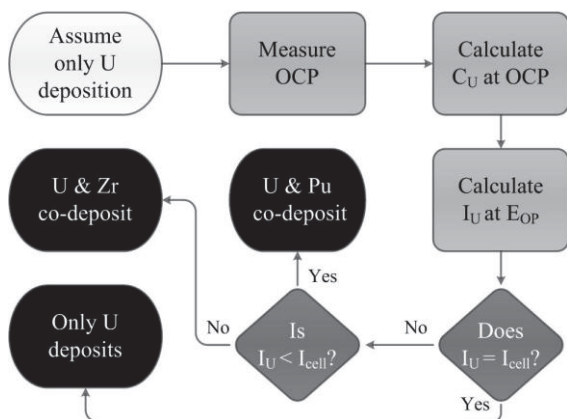


Figure 2 Method for determining depositing species

The co-depositing species (Pu or Zr) was determined by comparing  $I_U$  and  $I_{cell}$ . For example, if the model assumed only U deposition, but Pu had co-deposited, then the OCP of the cell would be more negative than expected. According to Eq.(15), a more negative OCP would predict a lower  $C_U$  resulting in an

underestimated  $I_U$ . Thus, if  $I_U$  was less than the ERAD calculated cell current, then Pu is the co-depositing species. The opposite would hold for Zr.

## II.B. Model Results

The performance of the proposed model was compared to ERAD by simulating an ER at varying salt compositions using the system parameters in Table I. The initial salt compositions for the U/Zr co-deposition and U/Pu co-deposition cases are displayed in Table II and III respectively. Pure uranium deposition is represented by Case 1 in Table II and Cases 1 and 2 in Table III..

Table I. Electrorefiner Parameters

Interfacial Area:		Initial Masses:	
Anode-Salt	3748 cm <sup>2</sup>	Anode	19.2 kg
Cathode-Salt	800 cm <sup>2</sup>	Salt	447 kg
Diffusion Layer Thickness:			
Anode	50 μm	Cathode	50 μm

Table II. Initial composition of molten salt in U/Zr co-deposition cases

Case	1	2	3	4
U (wt%)	7.567	6.567	5.567	4.567
Zr (wt%)	0.000	0.250	0.250	0.250
Pu (wt%)	0.234	0.234	0.234	0.234
Na (wt%)	1.520	1.520	1.520	1.520
Case	5	6	7	8
U (wt%)	7.567	4.567	7.567	6.567
Zr (wt%)	0.300	0.325	0.377	0.377
Pu (wt%)	0.234	0.234	0.234	0.234
Na (wt%)	1.520	1.520	1.520	1.520

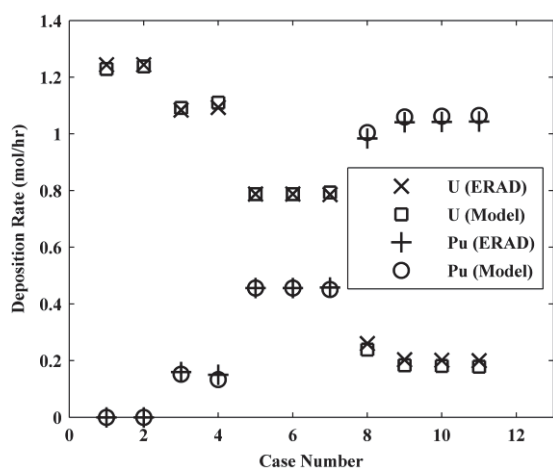
For each case, the operating temperature was set at 500 °C. The ER was set to operate at a cell current of 100 A and then stepped to 0, 5 and 100 A at an elapsed time of 2, 2.05 and 2.1 hrs respectively. The physical properties for each species were set to match the values reported by Hoover et. al.<sup>16</sup> with the exception of diffusion coefficients which are from Hoover et. al.<sup>17</sup> Additionally, a standard exchange current density of 0.8, 1.1 and 0.8 A/cm<sup>2</sup> was assumed for U, Pu, and Zr respectively. The anode in each case initially consisted of 84.6, 0.379, 11.5 and 3.55 wt% of U, Pu, Zr and Na respectively.

Table III. Initial composition of molten salt in U/Pu co-deposition cases

Case	1	2	3	4	5	6	7	8	9	10	11
U (wt%)	7.567	2.567	2.234	2.234	1.234	1.234	1.234	0.313	0.213	0.213	0.213
Pu (wt%)	0.234	0.234	0.567	2.567	3.234	5.567	7.567	4.234	4.234	5.567	7.234
Na (wt%)	1.520	1.520	1.520	1.520	1.520	1.520	1.520	1.520	1.520	1.520	1.520

The potentials calculated by ERAD at each current setting were recorded and fed to the model. Based on the current settings and their respective recorded potentials, the model determined the species depositing at the cathode and calculated the rate of deposition.

The deposition rates calculated in ERAD at the elapsed simulation time of 2 hrs were compared to the deposition rates determined by the model at the 100 A current setting. Plots comparing the deposition rates calculated by ERAD and the model for U/Pu and U/Zr co-deposition studies are found in Figure 3 and 4, respectively. In the plots, U deposition rates are represented by the boxes (new model) and x's (ERAD), while Pu or Zr deposition rates are represented by the circles (new model) and crosses (ERAD). On average, the errors of the predicted deposition rates for U and Pu relative to ERAD's calculations were 3.88% and 2.84% respectively. Likewise, the relative errors for U and Zr were 4.16% and 7.44%, respectively.



**Figure 3 Comparison of ERAD and model deposition rates for U and Pu**

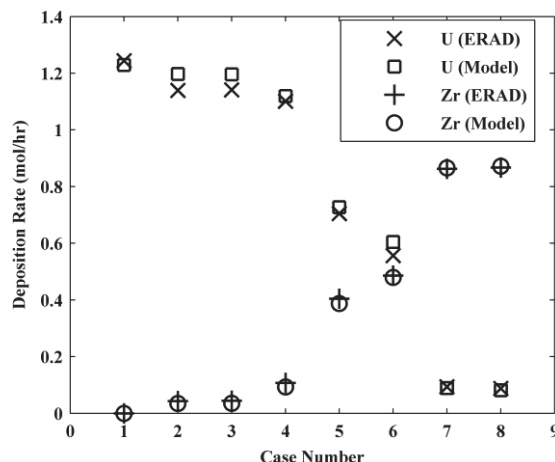


**Figure 4 Comparison of ERAD and model deposition rates for U and Zr**

### III. CONCLUSIONS

An inverse model was developed that used the cell current settings and cathode potential measurements to determine the species depositing on the cathode and their rates of deposition. The predicted deposition rates were comparable to those calculated by ERAD. On average, the predicted deposition rates had relative errors of 3.88% and 2.84% for U and Pu, respectively, in the case of U/Pu co-deposition and 4.16% and 7.44% for U and Zr, respectively, in the case of U/Zr co-deposition. Thus, the inverse model was able to predict the deposition rates without requiring information regarding the feed and salt composition, as the forward model, ERAD, does.

This model has the potential to be developed to provide real-time or near-real-time process monitoring of the cathode product which would aid in product optimization, process control and material accountability. However, an accurate mass-transfer correlation for the diffusion layer thickness specific to the ER of interest would need to be developed. Additionally, the effects of concentration variations on certain parameters, such as activity coefficients, would need to be determined.

### ACKNOWLEDGMENTS

This work was supported by the Russell Family Foundation. Additionally, Jun Li and David McNelis at UNC contributed their experience and technical expertise to this work. Special thanks to Supathorn Phongikaroon and Robert Hoover for their technical consulting.

## REFERENCES

1. C. H. ADAMS, J. C. BEITEL, G. BIRGERSSON, R. G. BUCHER, K. L. DERSTINE, and B. J. TOPPEL, "The Mass Tracking System – Computerized Support for MC&A and Operations at FCF," *Proc. of American Nuclear Society Topical Mtg. on DOE Spent Nuclear Fuel and Fissile Material Management*, Reno, Nevada, June 16-20, 1996, ANS (1996).
2. D. VADEN, "Fuel Conditioning Facility Electrorefiner Model Prediction versus Measurements," *Sep. Sci. Technol.*, 43, 9-10, 2684 (2008).
3. D. VADEN, "Fuel Condition Facility Electrorefiner Process Model," *Sep. Sci. Technol.*, 41, 10, 2003, (2006).
4. S. CHOI, J. PARK, K.-R. KIM, H. JUNG, I. HWANG, B. PARK, K. YI, H.-S. LEE, D. AHN, and S. PAEK, "Three-Dimensional Multispecies Current Density Simulation of Molten-Salt Electrorefining," *J. Alloys Compd.*, 503, 1, 177 (2010).
5. B. PARK, *A Time-Dependent Simulation of Molten Salt Electrolysis for Nuclear Wastes Transmutation (Doctoral dissertation)*, Ch. 3 and 4, Seoul National University, Seoul, South Korea (1999).
6. R. O. HOOVER, *Development of a Computational Model for the Mark-IV Electrorefiner (Master's thesis)*, University of Idaho, Idaho Falls, ID (2010).
7. J. LI, M.-S. YIM and D. MCNELIS, "A Comprehensive Electrorefining Process Simulation Model for Pyroprocessing of Spent Fuel," *Proc. GLOBAL 2011*, Makuhari, Japan, Dec. 11-16, 2011, Paper No. 472379 (2011).
8. J. H. LEE, K. H. OH, Y. H. KANG, S. C. HWANG, H. S. LEE, J. B. SHIM, E. H. KIM and S. W. PARK, "Assessment of a High-Throughput Electrorefining Concept for a Spent Metallic Nuclear Fuel—II: Electrohydrodynamic Analysis and Validation," *Nucl. Technol.*, 165, 3, 370 (2009).
9. J. ZHANG, "Possibility of Co-deposition of U and Pu at a Solid Cathode in Pyro-Chemical Processing," *Trans. Am. Nucl. Soc. (Vol. 106)*, Chicago, Illinois, June 24-28, 2012, ANS (2012).
10. R. M. CUMBERLAND, *Master's Thesis*. Korean Advanced Institute of Science and Technology. Daejeon, South Korea (In Progress).
11. M. IIZUKA, K. KINOSHITA, and T. KOYAMA, "Modeling of Anodic Dissolution of U-Pu-Zr Ternary Alloy in the Molten LiCl-KCl Electrolyte," *J. Phys. Chem. Solids*, 66, 2-4, 427 (2005).
12. T. KOYOMA, K. KINOSHITA, T. INOUE, M. OUGIER, R. MALMBECK, J.-P. GLATZ and L. KOCH, "Study of Molten Salt Electrorefining of U-Pu-Zr Alloy Fuel," *J. Nucl. Sci. Technol.*, Supplement 3, 765 (2002).
13. M. EISENBERG, C. W. TOBIAS and C. R. WILKE, "Ionic Mass Transfer and Concentration Polarization at Rotating Electrodes," *J. Electrochem. Soc.*, 101, 6, 306 (1954).
14. J.-Y. KIM, S.-E. BAE, D.-H. KIM, Y. S. CHOI, J.-W. YEON and K. SONG, "High-Temperature Viscosity Measurement of LiCl-KCl Molten Salts Comprising Actinides and Lanthanides," *Bull. Korean Chem. Soc.* 33, 11, 3871 (2012).
15. NATIONAL RESEARCH COUNCIL, *Electrometallurgical Techniques for DOE Spent Fuel Treatment: Final Report*, p. 31, The National Academy Press, Washington DC (2000).
16. R. O. HOOVER, S. PHONGIKAROON, M. F. SIMPSON, S. X. LI and T.-S. YOO, "Development of Computational Models for the Mark-IV Electrorefiner—Effect of Uranium, Plutonium, and Zirconium Dissolution at the Fuel Basket-Salt Interface," *Nucl. Technol.*, 171, 3, 276 (2010).
17. R. O. HOOVER, S. PHONGIKAROON, M. F. SIMPSON, T.-S. YOO and S. X. LI, "Computational Model of the Mark-IV Electrorefiner: Two-Dimensional Potential and Current Distributions," *Nucl. Technol.*, 173, 2, 176 (2011).